AD-782 262

INTERNAL WAVES RADIATED BY A MOVING SOURCE. VOLUME I. ANALYTIC SIMULATION

Michael Milder

R and D Associates

RDA-TR-2702-007

INTERNAL WAVES RADIATED BY A MOVING SOURCE
Volume I - Analytic Simulation

FEBRUARY 1974

By:
MICHAEL MILDER

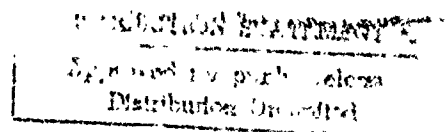The views and conclusions contained in this document
are those of the author and should not be interpreted
as necessarily representing the official policies,
either expressed or implied, of the Defense Advanced
Research Projects Agency or the United States Government.

R & D ASSOCIATES
Post Office Box 3580
Santa Monica,
California, 90403

525 WILSHIRE BOULEVARD ● SANTA MONICA ● TELEPHONE: (213) 451-5838

REPORT DOCUMENTATION PAGE

READ INSTRUCTIONS
BEFORE COMPLETING FORM

1. REPORT NUMBER	2. GOVT ACCESSION NO.	3. RECIPIENT'S CATALOG NUMBER
RDA-TR-2702-007		AD 782262

4. TITLE (and Subtitle)	5. TYPE OF REPORT & PERIOD COVERED
INTERNAL WAVES RADIATED BY A MOVING SOURCE Volume I - Analytic Simulation	Technical Report
	6. PERFORMING ORG. REPORT NUMBER

7. AUTHOR(s)	8. CONTRACT OR GRANT NUMBER(s)
MICHAEL MILDER	N00014-73-C-0105

9. PERFORMING ORGANIZATION NAME AND ADDRESS	10. PROGRAM ELEMENT, PROJECT, TASK AREA & WORK UNIT NUMBERS
R & D Associates P.O. Box 3850 Santa Monica, California 90403	

11. CONTROLLING OFFICE NAME AND ADDRESS	12. REPORT DATE
Defense Advanced Research Projects Agency 1400 Wilson Boulevard Arlington, Virginia 22209	February 1974
	13. NUMBER OF PAGES
	50

14. MONITORING AGENCY NAME & ADDRESS(if different from Controlling Office)	15. SECURITY CLASS. (of this report)
Office of Naval Research Department of the Navy Arlington, Virginia 22217	Unclassified
	15a. DECLASSIFICATION/DOWNGRADING SCHEDULE

16. DISTRIBUTION STATEMENT (of this Report)

17. DISTRIBUTION STATEMENT (of the abstract entered in Block 20, if different from Report)

18. SUPPLEMENTARY NOTES

19. KEY WORDS (Continue on reverse side if necessary and identify by block number)

NATIONAL TECHNICAL
INFORMATION SERVICE
U S Department of Commerce
Springfield VA 22151

20. ABSTRACT (Continue on reverse side if necessary and identify by block number)

An algorithm is derived for the efficient simulation of internal waves radiated from an object moving at constant speed in a medium of arbitrarily stratified density. The algorithm is based on a Fourier/normal-mode expansion of the linearized fluid equations in rectangular coordinates, and owes its efficiency to the Fast Fourier Transform used for numerical inversion of the analytically-derived field transforms. Sample calculations from a prototype computer program, XMODE, are described.

DD FORM 1473 EDITION OF 1 NOV 65 IS OBSOLETE.
1 JAN 73

TABLE OF CONTENTS

Preceding page blank   v

LIST OF FIGURES

LIST OF SYMBOLS

A	Body cross section
c	Phase speed
c_g	Group speed
E	Wake mixing efficiency
g	Acceleration of gravity
$G_{k,\omega}$	Vertical Green's function
$\vec{k}, k, k_x, k_y$	Horizontal vector wavenumber, modulus, and components
K_ϵ	Eddy diffusion constant for turbulent wake
K_1	Wake entrainment constant
L	Body length
m, n	Mode index
N	Vaisala frequency
N_m	Vertical mode-averaged N
p	Pressure per unit density
P_m	Equivalent vertical wavenumber for mode m
Q	Kinematic wake quadrupole moment
q_m	Total wavenumber for mode m
R	Wake radius
R_b	Maximum body radius
$\dot{R}$	Wake entrainment velocity
s	Displacement source function
t	Time
$\vec{u}, u_x, u_y$	Horizontal vector velocity and components

u'	Wake turbulent velocity scale
v	Source speed
V	Body volume
x, y, z	Cartesian coordinates (track, crosstrack, and negative depth)
z_o	Source depth
Z_a	Active thermocline depth: $N = 0$ for $z < - Z_a$
$(\bar{})$	Fourier transform with respect to x and y
$(\tilde{})$	Fourier transform with respect to y
α	Relative density gradient inside wake
β	Ambient relative density gradient
γ	Inverse phase speed
δ	Dirac delta-function
Δ	Function describing $\Delta\zeta$, below
ε	Horizontal strain, and turbulent eddy diffusivity
ε_t	Horizontal strain rate
∇'	Horizontal vector gradient
ϕ	Normal-mode eigenfunction
ϕ'	$\partial\phi/\partial z$
ρ	Fluid density
ξ	Horizontal vector field displacement
ζ	Vertical field displacement
$\Delta\zeta$	Displacement of equilibrium level due to density redistribution in wake
ω	Radian frequency

SECTION 1. GENERAL DESCRIPTION

1.1 INTRODUCTION

Present methods for predicting internal wave fields produced by objects moving in stratified media are limited in their physical realism, flexibility, and economy. Recent efforts to define standards for internal-wave prediction have helped to clarify the shortcomings of existing techniques, which occur in one or more of the following areas:

- Modelling the dynamics of turbulent wake growth, buoyancy transport, and wake collapse.

- Modelling the propagation of radiated internal waves in a medium of arbitrary buoyancy stratification.

- Maintaining numerical precision and stability in a field calculation encompassing a wide range of horizontal and vertical length scales, at acceptable computing cost and speed.

Some of these shortcomings are fundamental and unavoidable, while some are accidental, depending on the approach used. For example, a three-dimensional finite-difference calculation, superior for near-field flow and wake dynamics, is severely limited in the upper length and time scales it can achieve, simply because of limits on available computer storage, speed, and accuracy. On the other hand, limitations in existing analytic approaches can be overcome. One such approach now in use by TRW employs a three-layer model of density stratification that is too simplified to reproduce wave propagation on real thermoclines, although it is perfectly adequate for its original purpose, which was to provide estimates of field magnitudes and shapes [2].

1

A more general analytic code can be envisioned, one based on a Fourier/normal-mode expansion of the linearized field equations for an arbitrary profile of stratified buoyancy, that would meet the requirements for generality, scale and efficiency. Like its predecessors, however, such a code would have to depend on parametric source models to represent the excitation of internal waves by the moving body and collapsing wake, source models that will have to be devised and validated elsewhere.

A two-fold approach has been suggested [3] in which an efficient code of the analytic type is developed for routine simulations, while at the same time a "research" code of the finite-difference type is developed to provide validated source models for the analytic code.

This two-volume report describes a prototype analytic code, XMODE, which has been developed at RDA to provide inexpensive simulations of radiated internal-wave fields in a variety of realistic thermoclines. XMODE represents an improvement over existing codes in two important respects: it contains an efficient eigenfunction generator for the normal-mode analysis of an arbitrary input density profile, and it abandons the stationary-phase method of field calculation in favor of a more nearly exact, and very rapid, inversion in rectangular coordinates via the Fast Fourier Transform [4].

Volume I contains a general description of XMODE and a detailed derivation of the algorithm for representative body and wake sources. Volume II is a user's guide to XMODE, containing a description of the computer routines, operating instructions, and FORTRAN listings.

2

Some of the procedures and computer subroutines, those having to do with eigenfunction generation, are identical to those in the computer code ZMODE, which is an integral part of XMODE and which has been described fully in an earlier report [1]. This material is not duplicated here; potential users of XMODE should obtain Reference 1 as a companion volume to the present report.

1.2 OUTLINE OF METHOD

The algorithm used by XMODE is based on a Fourier/normal-mode expansion of the linearized equations of stratified flow, with simple local sources. As in other formulations the transformed solution is obtained as an algebraic combination of eigenfunction amplitudes and dispersion quantities. However, the present formulation is distinct in that the transform is inverted in rectangular coordinates, first along the x-direction (track) by analytic means, then along the y-direction (crosstrack) by a numerical Fast Fourier Transform (FFT). The partial crosstrack transforms obtained in the first step for each normal mode are complex functions whose amplitudes are invariant with respect to x and whose complex phases are linearly proportional to x. This property allows the partial transforms to be assembled rapidly from independent amplitude and phase factors computed and stored ahead of time. At each value of x the numerical phase-and-sum operation is, for twenty modes, no more time-consuming than the FFT computation of the crosstrack field, so that the full efficiency of the FFT is realized.

1.3 ADVANTAGES AND LIMITATIONS

The logic of XMODE is designed for efficient computation of radiated internal wave field properties at the ocean surface, or on a horizontal plane (x-y) at any specified depth. Computation of the field on the vertical crossplane (y-z) is somewhat less efficient, and computation on a vertical plane (x-z) is least efficient of all. All points in the plane

3

are computed with equal precision; unlike previously used stationary-phase methods, the FFT in rectangular coordinates has no difficulty with points on or near the coordinate axes ($x = 0$ and $y = 0$) originating on the source.

Other specific assumptions and features are:

- Linearized fluid equations with dipole body and quadrupole wake sources.

- Choice of field quantity among vertical displacement, scalar strain, x- and y- components of velocity, and scalar strain rate.

- No ambient shear flow.

- No vertical momentum in wake.

- Source speed must exceed maximum ambient phase speed (Super-Froude source).

4

SECTION 2. SPECIFICATIONS OF THE XMODE CODE AND SAMPLE CALCULATIONS

2.1 RESOLUTION AND DYNAMIC RANGE

Each crosstrack field contains 256 physical resolution elements Δy,

$$\text{field half-width} = 256 \cdot \Delta y;$$

the width and resolution size are somewhat adjustable, but Δy, which should approximate the reciprocal of the upper wavenumber limit in the ZMODE calculation, is constrained by numerical stability considerations to

$$\Delta y \gtrsim Z_a/15 ,$$

where Z_a is the total depth of the active thermocline. For $Z_a = 300$ m this permits a crosstrack resolution of 20 m and a field half-width of 5120 m. The number of points calculated per crosstrack field is optional among 256, 512, 1024, and 2048, for redundant sampling at multiples of 2, 4, and 8 times the Nyquist frequency Δy^{-1}.

Any number of equally-spaced crosstrack fields can be requested in a given calculation, with an arbitrary track spacing Δx.

The maximum number of normal modes is 20, so that the effective vertical resolution is $\Delta Z \approx Z_a/20$.

Since the source transforms are generated directly from analytic formulas and stored in floating-point format the effective dynamic range of the tabulated transforms is very large, limited only by the eigenmode convergence precision of ZMODE, which is in the neighborhood of 10^{-20}, or double the eigenvalue convergence precision.

Errors introduced by the finite, discrete FFT are of two simple types: accumulated roundoff, which is a few times machine precision, and aliasing, which superposes fields from image sources spaced at multiples of the field width from the actual track. The image fields are negligible so long as the simulation time is short compared to the time required for the fastest propagating field components to traverse a half-width; when this artificial periodicity is taken into account, the images will not affect estimates of the spectral content, which can be recovered with a precision of 10^{-13}.

2.2 CORE REQUIREMENTS AND EXECUTION TIMES

The XMODE source deck contains 1120 cards. On the CDC 7600, both the RUN compiler and the FTN optimizing compiler produce an object code occupying less than 60,000 words (162,000 octal).

The execution times are proportional to the number of modes requested in a calculation. The values listed below are for the full 20 modes.

Execution Times, Seconds

Procedure	Module	RUN	FTN
● Dispersion Tables and Mode Amplitudes	ZMODE	11.2	6.6
● Recalculate with new Source Depth	ZMODE	4.1	2.5
● Crosstrack Source Transforms	SOURCE	0.02	0.01
● With Printer Plots	SOURCE	0.30	0.38
● Radiated field on 100(x) by 1024(y) array	XFIELD	6.4	5.3

Particularly noteworthy is the efficiency achieved by the XFIELD module. Of the 64 milliseconds computation time per 1024-point crosstrack field (RUN compiler), half is devoted to the 20-mode phase-and-sum, and half to the FFT.

The computation time of the dispersion tables, the most time-consuming operation, will depend also on the chosen number of eigenmode integration steps, the convergence precision, and tabular wavenumber density; the values 200, 10^{-10}, and 41 used in the test case are felt to be typical for deep-ocean calculations. For a series of field calculations with differing source speed or field type, a single dispersion calculation suffices. A change in source or field depth requires a new calculation of .ne eigenfunctions so that the mode amplitudes at the new depths can be tabulated. When converged eigenvalues are already present the eigenvalue search can be bypassed, shortening the (RUN) time from 11.2 to 4.1 seconds, as indicated.

2.3 SAMPLE CALCULATIONS

The sample calculations illustrated below simulate a source 60 meters deep moving at 2.0 kt and 16 kt. The depth chosen places the source 15 meters below the sharply eroded boundary of the test thermocline, shown in Figure 2-1, which has been taken from data obtained on the oceanographic research vessel FLIP. The corresponding profile of Vaisala frequency and the ZMODE-derived internal wave dispersion plot are shown in Figures 2-2 and 2-3.

The crosstrack source transforms computed by the SOURCE module are available in numerical and graphical output. Figure 2-4 is a sample of the numerical output, which includes transform amplitude versus both the scalar

wavenumber, k, and its crosstrack component, k_y. The graphical output, Figures 2-5 and 2-6, plots the squared transform amplitude against k_y. These two examples show the modal energy spectra of crosstrack surface current for the first six modes at 2.0 kt and 16.0 kt respectively. For greater clarity, the usual XMODE printer-plot subroutine has been replaced by an equivalent pen-plot routine specific to the RDA plotting hardware. The low-speed and high-speed cases are dominated respectively by body and wake excitation; note the flat spectra characteristic of the latter and peaked spectra of the former, especially in the first mode, where the low-wavenumber components, whose phase speed is about 1.6 kt, are nearly resonant at 2.0 kt.

The output of the field calculation in XFIELD is placed directly on magnetic tape. At the same time XFIELD generates a summary printout, as in Figure 2-7, containing the peak amplitude and corresponding location for each crossfield. The boundary amplitudes are useful at short simulation times as an indication of the transform roundoff and aliasing errors.

Figures 2-8 and 2-9 are raster plots made directly from the sample calculation output tape, depicting crosstrack surface current associated with the radiated internal waves in modes 1-20. Plot ranges of 0-2.0 km and 0-750 m crosstrack are used for the 2.0 kt and 16.0 kt cases, respectively, or 40% and 15% of the calculated field, for best rendering of the features. The downtrack coordinate is in time units, for both cases spanning 5000 sec in increments of 50 sec.
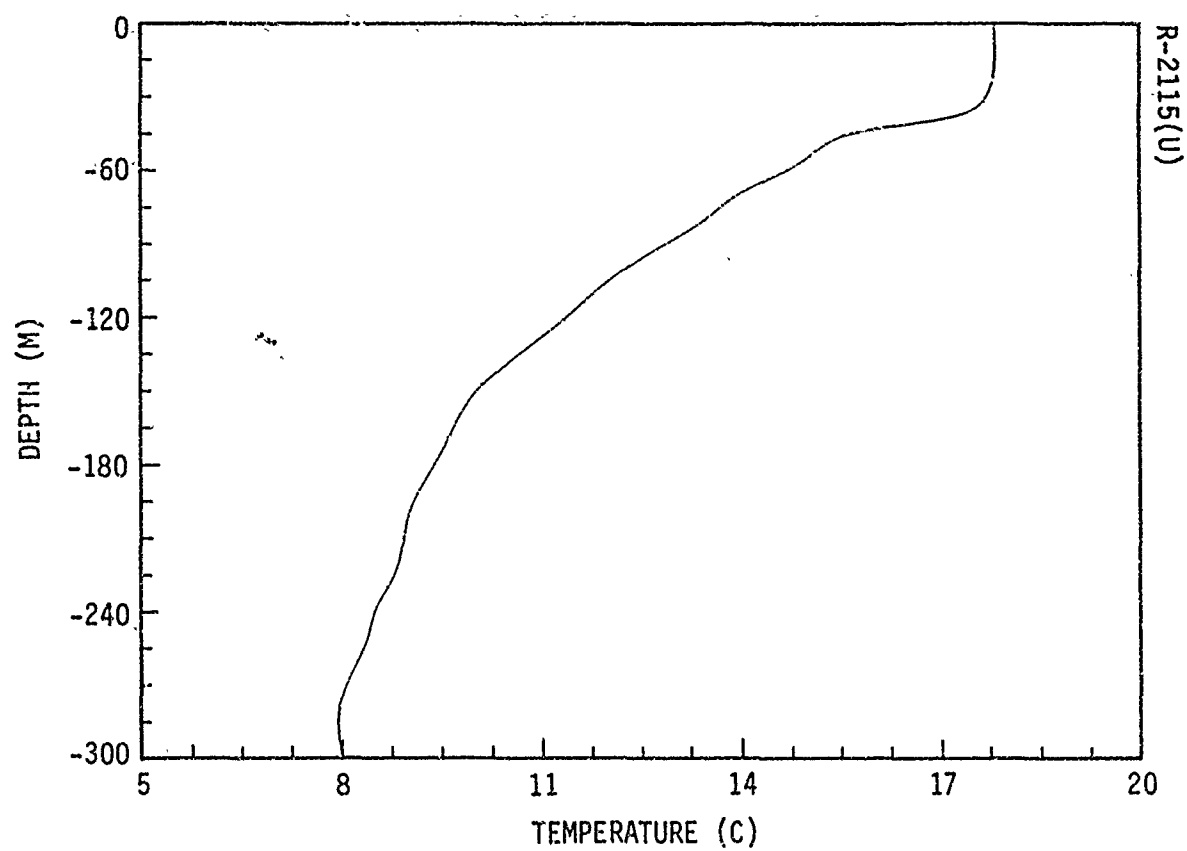
Figure 2-1. Temperature vs Depth Profile for Thermocline
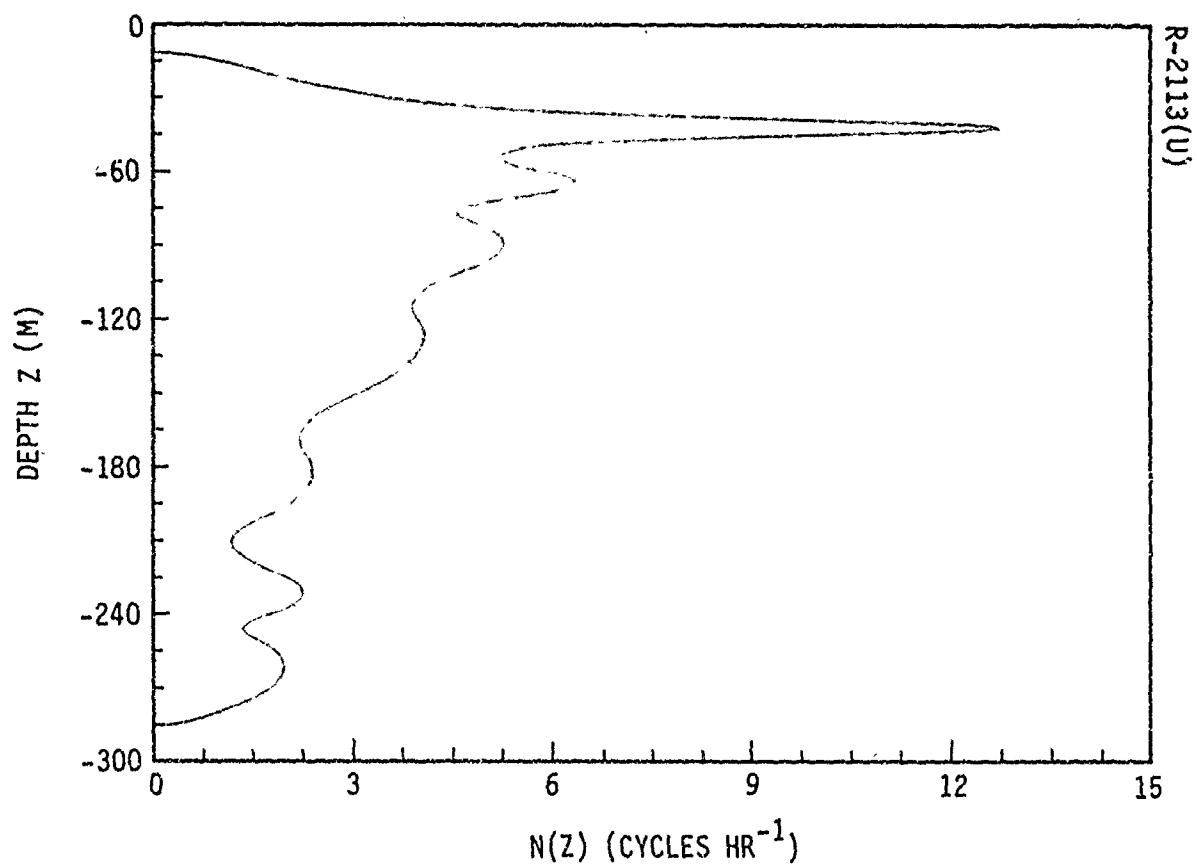Used in Sample Calculations

Figure 2-2. Vaisala Frequency $N(z) = [-(g/\rho)d\rho/dz]^{1/2}$ for Temperature Profile of Figure 2-1
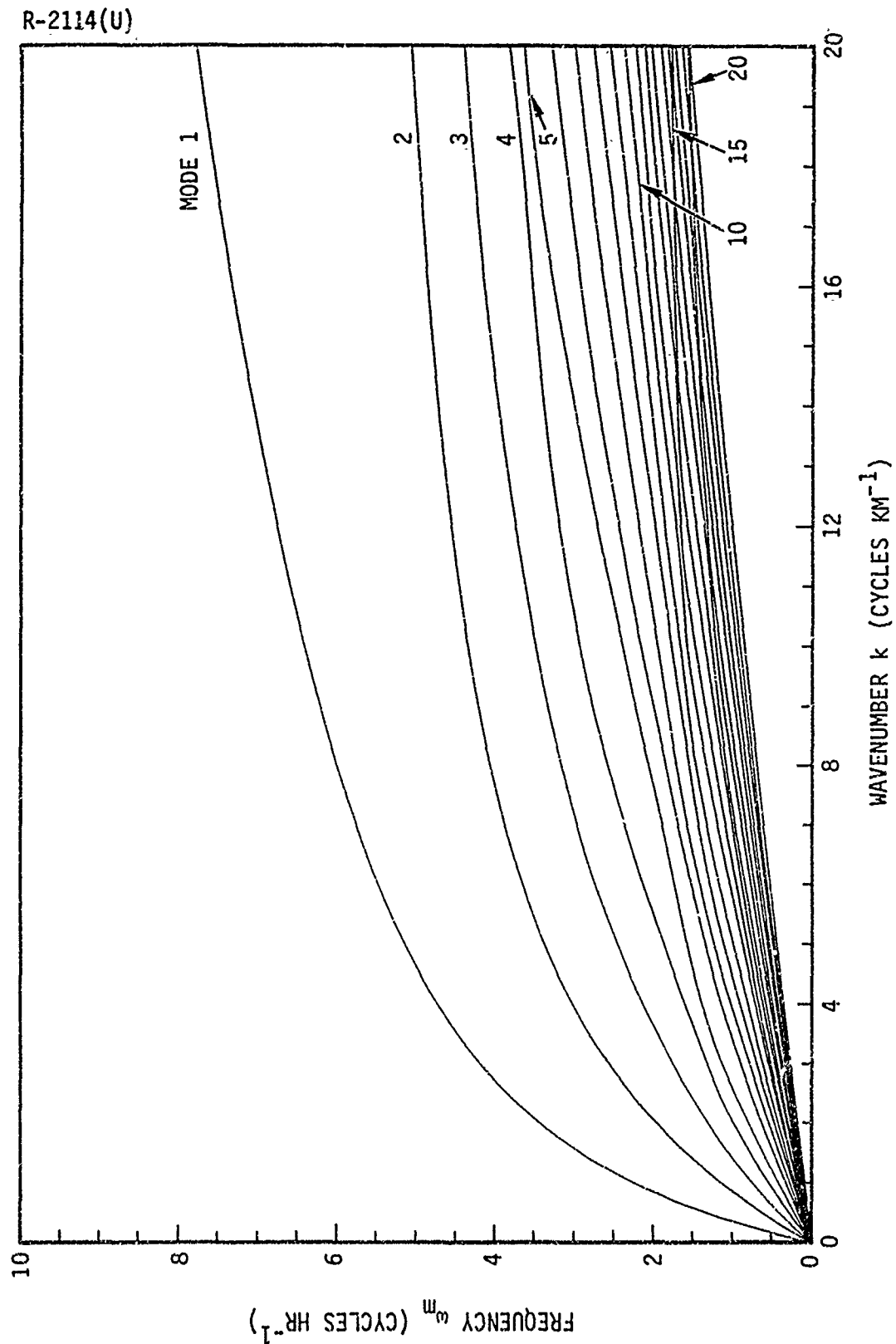
10

R-2114(U)

Figure 2-3. Normal-Mode Dispersion Frequencies $\omega_m(k)$ for Sample Thermocline

11

*** SQUARED CROSSTRACK TRANSFORM ***

MODE 3   QUANTITY -- UY

K CY/KM	KY CY/KM	BODY (Q*M)**2	WAKE (Q*M)**2
0.000	0.000	0.	1.406E-06
.500	.488	2.900E-05	1.294E-06
1.000	.980	7.000E-05	1.156E-06
1.500	1.473	9.823E-05	1.088E-06
2.000	1.969	1.158E-04	1.060E-06
2.500	2.466	1.235E-04	1.017E-06
3.000	2.963	1.212E-04	9.315E-07
3.500	3.461	1.108E-04	8.153E-07
4.000	3.959	9.578E-05	6.895E-07
4.500	4.457	7.939E-05	5.690E-07
5.000	4.956	6.369E-05	4.616E-07
5.500	5.455	4.980E-05	3.696E-07
6.000	5.955	3.816E-05	2.929E-07
6.500	6.454	2.878E-05	2.302E-07
7.000	6.954	2.142E-05	1.796E-07
7.500	7.454	1.577E-05	1.392E-07
8.000	7.954	1.150E-05	1.071E-07
8.500	8.455	8.320E-06	8.181E-08
9.000	8.955	5.965E-06	6.198E-08
9.500	9.455	4.238E-06	4.651E-08
10.000	9.956	2.982E-06	3.452E-08
10.500	10.456	2.075E-06	2.531E-08
11.000	10.957	1.425E-06	1.829E-08
11.500	11.457	9.658E-07	1.301E-08
12.000	11.957	6.441E-07	9.100E-09
12.500	12.458	4.219E-07	6.241E-09
13.000	12.958	2.708E-07	4.188E-09
13.500	13.459	1.698E-07	2.742E-09
14.000	13.959	1.036E-07	1.744E-09
14.500	14.460	6.104E-08	1.071E-09
15.000	14.960	3.444E-08	6.296E-10
15.500	15.461	1.833E-08	3.487E-10
16.000	15.961	8.960E-09	1.773E-10
16.500	16.462	3.824E-09	7.864E-11
17.000	16.962	1.266E-09	2.703E-11
17.500	17.463	2.160E-10	4.792E-12
18.000	17.963	3.175E-12	7.307E-14
18.500	18.463	2.163E-10	5.162E-13
19.000	18.964	6.140E-10	1.519E-11
19.500	19.464	1.062E-09	2.721E-11
20.000	19.965	1.492E-09	5.957E-11

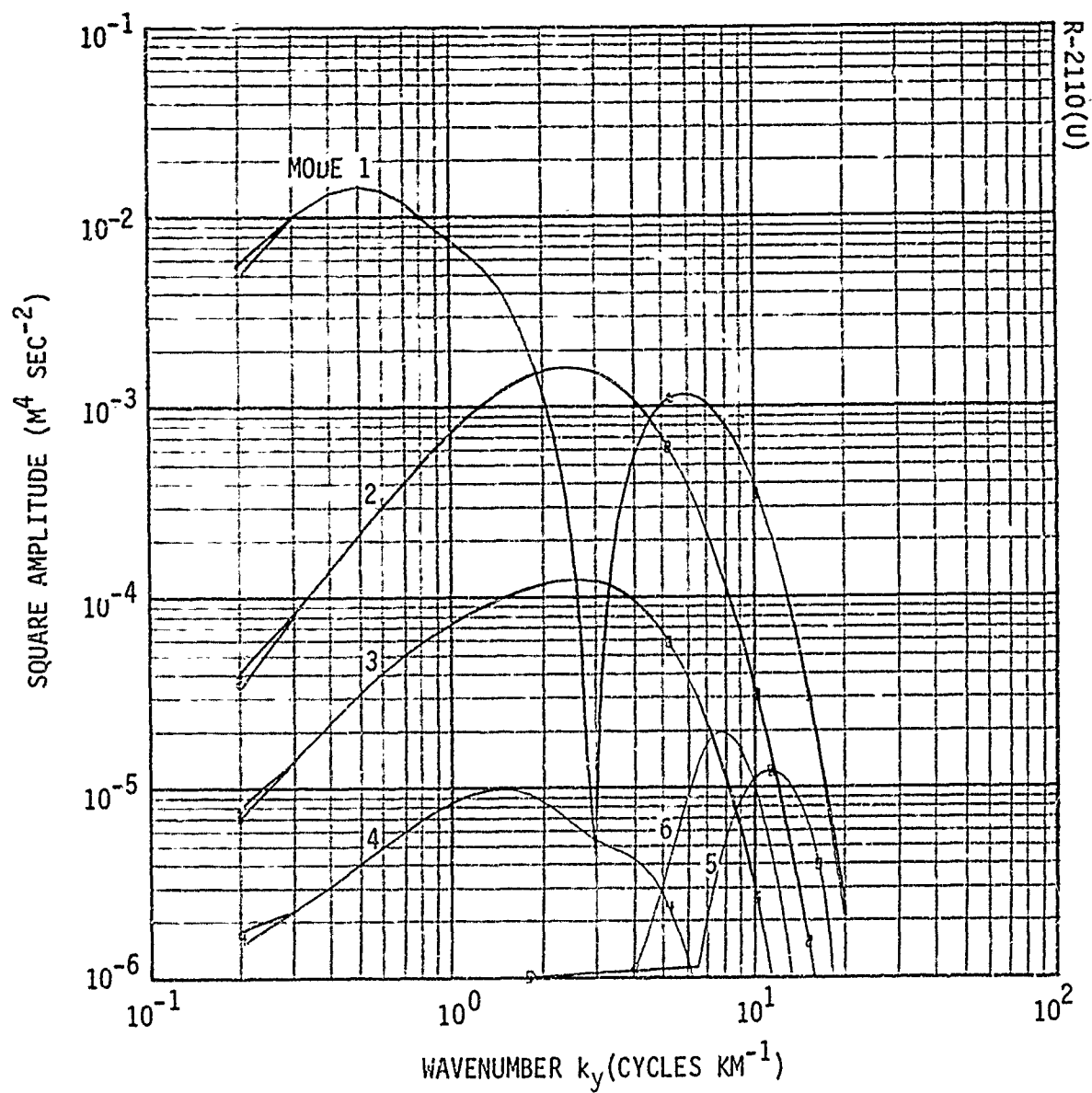Figure 2-4. Sample SOURCE Module Printout for Mode 3, Source Speed 2.0 Kt

Figure 2-5. Excitation Spectra of Surface Crosstrack Velocity (Squared Source Transforms) for Modes 1-6, Source Speed 2.0 Kt
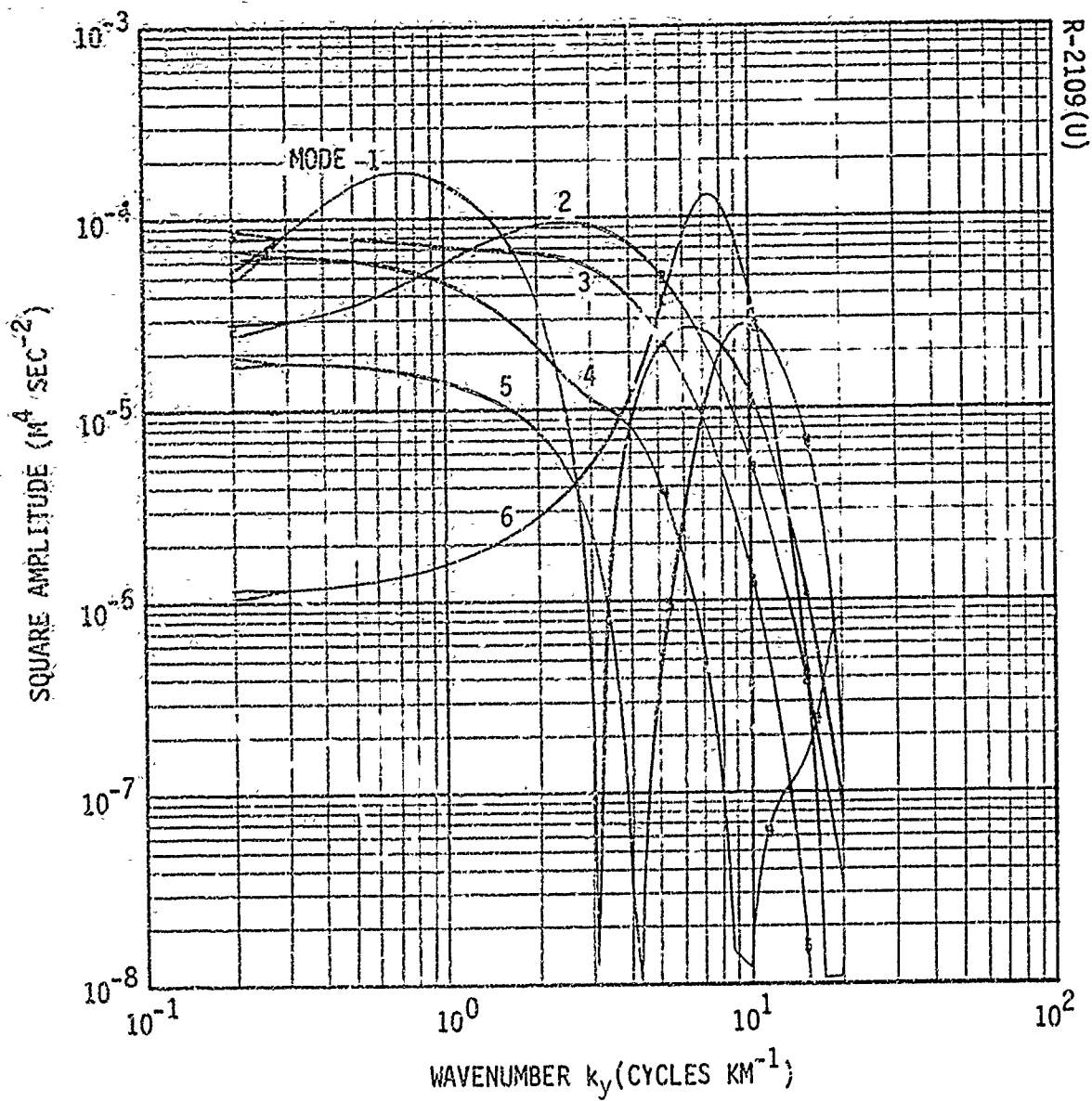
Figure 2-6. Excitation Spectra of Surface Crosstrack Velocity (Squared Source Transforms) for Modes 1-6, Source Speed 16.0 Kt

*** FIELD OUTPUT SUMMARY ***

* QUANTITY   UY
* SPEED, KT 16.00
* DEPTH, M 60.0
* XMAX*WIDTH 205

TIME, SEC	TRACK, M	PEAK SIGNAL	AT Y, M	BOUNDARY
50.0	411.5	1.137E-04	30.0	1.806E-10
100.0	823.1	1.292E-04	30.0	1.391E-10
150.0	1234.6	1.196E-04	35.0	1.211E-10
200.0	1646.2	1.022E-04	45.0	1.289E-10
250.0	2057.7	9.696E-05	60.0	1.601E-10
300.0	2469.3	1.144E-04	90.0	2.116E-10
350.0	2880.8	1.337E-04	95.0	2.787E-10
400.0	3292.4	1.488E-04	95.0	3.545E-10
450.0	3703.9	1.564E-04	95.0	4.307E-10
500.0	4115.4	1.580E-04	100.0	4.986E-10
550.0	4527.0	1.527E-04	100.0	5.502E-10
600.0	4938.5	1.425E-04	105.0	5.788E-10
650.0	5350.1	1.293E-04	105.0	5.792E-10
700.0	5761.6	1.143E-04	110.0	5.474E-10
750.0	6173.2	9.915E-05	110.0	4.794E-10
800.0	6584.7	8.449E-05	115.0	3.710E-10
850.0	6996.2	7.747E-05	160.0	2.174E-10
900.0	7407.8	7.267E-05	160.0	1.331E-11
950.0	7819.3	6.906E-05	220.0	2.462E-10
1000.0	8230.9	6.571E-05	225.0	5.649E-10
1050.0	8642.4	8.376E-05	30.0	9.453E-10
1100.0	9054.0	1.129E-04	30.0	1.388E-09
1150.0	9465.5	1.444E-04	35.0	1.894E-09
1200.0	9877.1	1.775E-04	40.0	2.463E-09
1250.0	10288.6	2.099E-04	45.0	3.098E-09
1300.0	10700.1	2.368E-04	50.0	3.802E-09
1350.0	11111.7	2.553E-04	50.0	4.591E-09
1400.0	11523.2	2.683E-04	55.0	5.443E-09
1450.0	11934.8	2.712E-04	60.0	6.394E-09
1500.0	12346.3	2.656E-04	60.0	7.442E-09
1550.0	12757.9	2.588E-04	65.0	8.592E-09
1600.0	13169.4	2.448E-04	70.0	9.852E-09
1650.0	13581.0	2.310E-04	70.0	1.123E-08
1700.0	13992.5	2.159E-04	70.0	1.273E-08
1750.0	14404.0	2.043E-04	70.0	1.438E-08
1800.0	14815.6	1.991E-04	75.0	1.619E-08
1850.0	15227.1	2.008E-04	75.0	1.818E-08
1900.0	15638.7	2.066E-04	75.0	2.040E-08
1950.0	16050.2	2.144E-04	80.0	2.286E-08
2000.0	16461.8	2.248E-04	80.0	2.562E-08
2050.0	16873.3	2.385E-04	85.0	2.871E-08
2100.0	17284.8	2.548E-04	90.0	3.218E-08
2150.0	17696.4	2.730E-04	95.0	3.610E-08
2200.0	18107.9	2.908E-04	100.0	4.033E-08
2250.0	18519.5	3.058E-04	100.0	4.555E-08
2300.0	18931.0	3.212E-04	105.0	5.125E-08
2350.0	19342.6	3.282E-04	110.0	5.771E-08
2400.0	19754.1	3.341E-04	110.0	6.505E-08
2450.0	20165.7	3.353E-04	115.0	7.335E-08
2500.0	20577.2	3.377E-04	115.0	8.274E-08

Figure 2-7. Sample Summary Printout From XFIELD Module

Figure 2-8. Raster Plot of Crosstrack Surface Current U_y for 2.0 Kt Source Speed. Interline Space Represents Amplitude of $0.01 cm sec^{-1}$. Track Length Depicted is 6.14 Km.

R-2112(U)
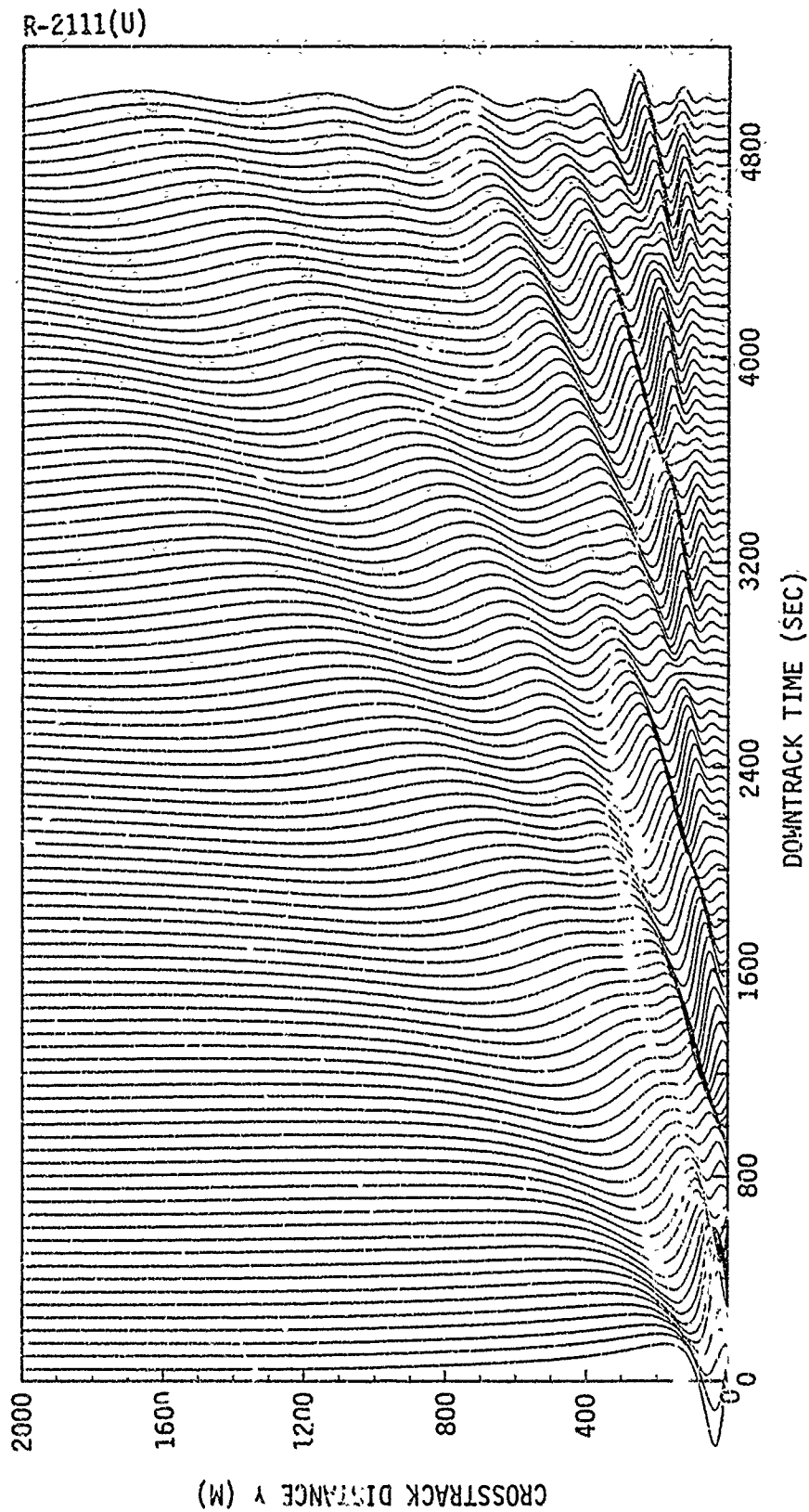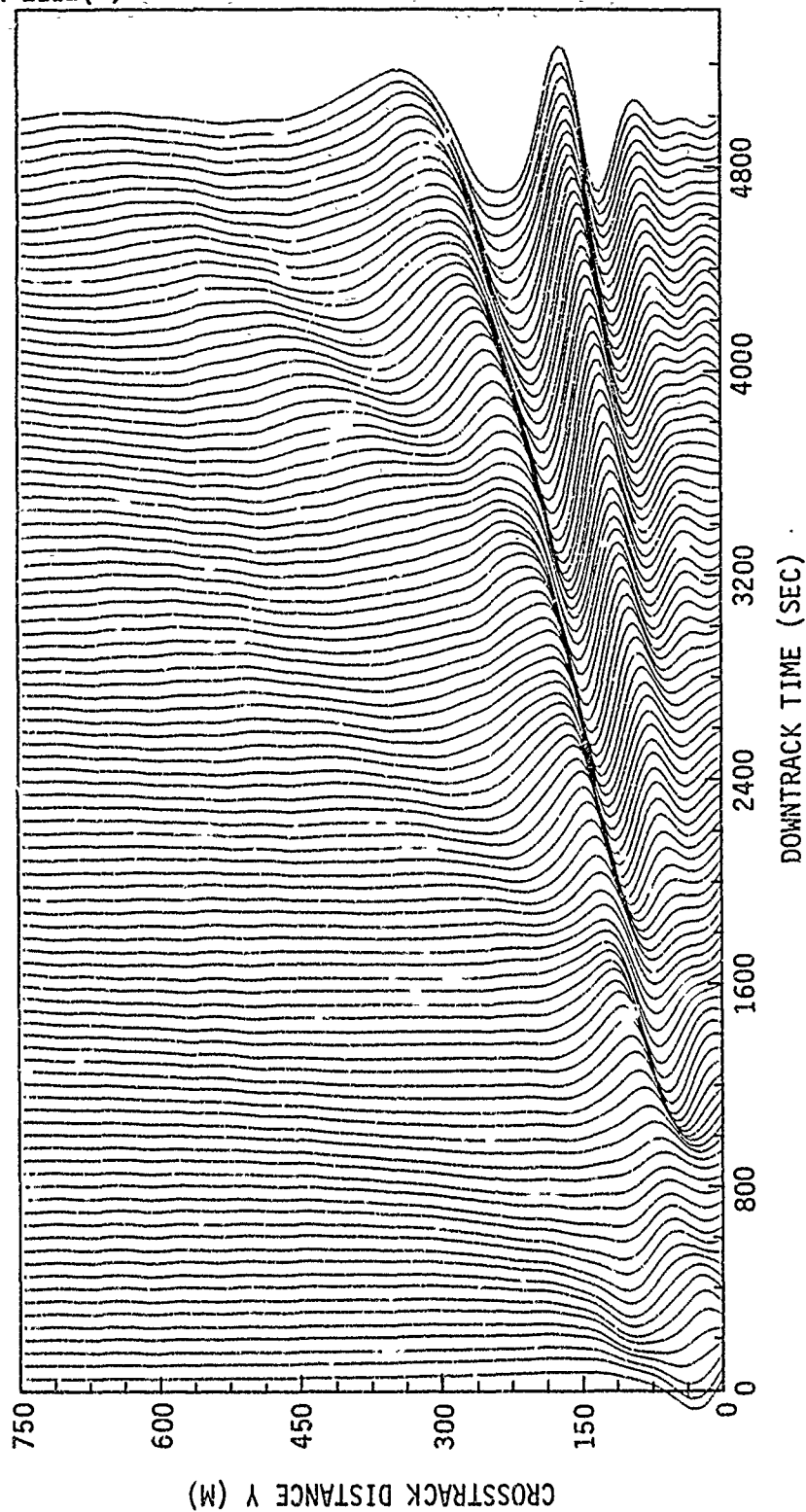

Figure 2-9. Raster Plot of Crosstrack Surface Current U for 16.0 Kt Source Speed. Interline Space Represents Amplitude of 0.005y cm sec^{-1}. Track Length Depicted is 41.2 Km.

17

SECTION 3. BODY-GENERATED WAVES

Internal waves are generated in an incompressible, stratified fluid when a moving object displaces the level surfaces from equilibrium. If the radiated displacement amplitudes are small, and if the traverse time of the object is short compared to the time scale associated with stratification, then the excited field is well described by linearized equations with a simple set of singular displacement sources. The one approximation that may be unrealistic for certain cases is the neglect of ambient current shear.

The following normal-mode analysis of body-generated radiation is similar to the general treatment of Miles [5]. Certain differences of format are dictated by the rectangular coordinates chosen for ease of computation, and these will be pointed out as they are introduced.

3.1 EQUATIONS OF MOTION

The coordinates are x (track), y (cross-track), and z (depth, positive upward, zero at surface). The fluid displacement from equilibrium will be described by a vertical component ζ and a two-component vector ξ in the horizontal plane. In the usual Boussinesq approximation with small displacements and small departures p from equilibrium pressure, the equations of motion are

$$\ddot{\zeta} + \frac{\partial p}{\partial z} + N^2(z) \, \zeta = 0 \qquad (3-1)$$

$$\ddot{\xi} + \nabla' p = 0 \qquad (3-2)$$

where ∇' stands for the horizontal gradient $(\partial/\partial x, \partial/\partial y)$ and N is the Vaisala frequency associated with the buoyancy stratification

$$N^2 = -\frac{g}{\rho} \frac{d\rho}{dz} . \qquad (3-3)$$

Conservation of volume will be modified to include a local set of sources and sinks describing the moving body,

$$\frac{\partial \zeta}{\partial z} + \nabla' \xi = s(x-vt, y, z) . \tag{3-4}$$

To eliminate the pressure, we apply $\partial/\partial z$ to (3-2), ∇' to (3-1), and subtract,

$$\nabla' \ddot{\zeta} + N^2 \nabla' \zeta - \frac{\partial \ddot{\xi}}{\partial z} = 0 ; \tag{3-5}$$

we can then eliminate the ξ term by taking the horizontal divergence of (3-5) and adding the result of $(\partial/\partial z) (\partial^2/\partial t^2)$ on (3-4),

$$\left(\nabla'^2 + \frac{\partial^2}{\partial z^2} \right) \ddot{\zeta} + N^2 \nabla'^2 \zeta = \frac{\partial \ddot{s}}{\partial z} \tag{3-6}$$

3.2 NORMAL MODE SOLUTION IN FOURIER-TRANSFORM COORDINATES

Using the notation ($^-$) for the 2-dimensional Fourier transforms in the horizontal plane

$$\zeta(\vec{k},z) = \int e^{i k \cdot x} \zeta \, dx dy \tag{3-7}$$

and so on, with $k \cdot x \equiv k_x x + k_y y$, and observing that every component of a steady solution emanating from the moving source (3-4) must have the particular time dependence

$$\zeta(\vec{k},z) \, e^{i \omega t} , \quad \omega \equiv k_x v, \tag{3-8}$$

we get from (3-6)

$$\frac{\partial^2 \bar{\zeta}}{\partial z^2} + k^2 \left(\frac{N^2}{\omega^2} -1 \right) \bar{\zeta} = \frac{\partial \bar{s}}{\partial z} , \tag{3-9}$$

where $k^2 = k_x^2 + k_y^2$ and $\bar{s}$ is the transform of s at $t = 0$.

20

At each value of $\vec{k}$, the solution $\overline{\zeta}$ to the inhomogeneous equation above can be obtained as a linear combination of the eigensolutions ϕ_m of the corresponding homogeneous equation

$$\frac{\partial^2 \phi_m}{\partial z^2} + k^2 \left(\frac{N^2}{\omega_m^2} - 1 \right) \phi_m = 0, \quad m = 0, 1, 2, \ldots \qquad (3\text{-}10)$$

which define the freely propagating normal modes. The functions ϕ_m vanish at $z = 0^*$ and at $z = b$, the ocean bottom. They form a complete orthogonal set,

$$\int_{-b}^{o} \phi_n N^2 \phi_m \, dz = \delta_{nm}, \qquad (3\text{-}11)$$

over the vertical interval in which $N(z)$ is nonvanishing. In these defining equations the scalar wavenumber is a continuous parameter upon which the functions ϕ_m and the eigenvalues ω_m depend, a convention opposite to that of Miles' treatment, in which k is the eigenvalue and ω the parameter. The present choice simplifies the logic of the numerical algorithm.

We now proceed in the usual way to assemble the eigenfunctions into a Green's function $G_{k,\omega}(z, z_0)$ for (3-9),

$$\left[\frac{\partial^2}{\partial z^2} + k^2 \left(\frac{N^2}{\omega^2} - 1 \right) \right] G_{k,\omega} = \delta(z - z_0), \qquad (3\text{-}12)$$

---

*Coupled displacements of the free surface are very small and can be safely neglected. See Phillips [6].

21

which in combination with the source transform $\partial \bar{s}/\partial z$ will yield the displacement transform $\bar{\zeta}$. The identity

$$\sum_{m=1}^{\infty} \phi_m(z) \ \phi_m(z_o) \ N^2(z) = \delta(z - z_o) \qquad (3\text{-}13)$$

and the property, via equation (3-10),

$$\left[\frac{\partial^2}{\partial z^2} + k^2 \left(\frac{N^2}{\omega^2} - 1\right)\right] \phi_m = k^2 N^2 \left(\frac{1}{\omega^2} - \frac{1}{\omega_m^2}\right) \phi_m$$

together imply

$$G_{k,\omega}(z,z_o) = -\frac{\omega^2}{k^2} \sum_{m=1}^{\infty} \frac{\omega_m^2}{\omega^2 - \omega_m^2} \ \phi_m(z) \ \phi_m(z_o). \qquad (3\text{-}14)$$

To represent the effect of a cylindrically symmetric body we distribute displacement sources along the submerged track $z = z_o$, $y = 0$,

$$s(x,y,z) = A(x) \ \delta(y) \ \delta(z - z_o);$$

the particular choice

$$A(x) = \begin{cases} \text{const.,} & |x| \leq L/2 \\ 0, & |x| > L/2 \end{cases}$$

is equivalent to the Rankine ovoid of volume $V = AL$ and dipole length L (except for the effects of local stratification and the rigid surface in distorting the boundary streamlines). For this choice, the source transform term in (3-9) is

$$\frac{\partial \bar{s}}{\partial z}(\vec{k}, z) = V \frac{\sin k_x L/2}{k_x L/2} \delta'(z - z_o) \qquad (3-15)$$

where the prime (') is used here and subsequently to denote differentiation by z. For cases of practical interest the values of $k_x = \omega_m/v$ present in the radiated field will be such that

$$\frac{k_x L}{2} < \frac{NL}{2v} \ll \pi$$

so that the form factor will be very nearly unity; note that this inequality must hold also for the distortions in the Rankine ovoid boundary streamlines to remain small. The body is therefore effectively a point monopole for displacement (or point dipole for velocity). The equation for the displacement transform then becomes

$$\left[\frac{\partial^2}{\partial z^2} + k^2 \left(\frac{N^2}{\omega^2} - 1 \right) \right] \bar{\zeta} = V \delta'(z - z_o) \qquad (3-16)$$

so that $\bar{\zeta}$ is minus V times the derivative with respect to z_o of the Green's function (3-14),

$$\overline{\zeta}(\vec{k},z) = \frac{v}{k^2} \sum_{m=1}^{\infty} \frac{\omega^2 \omega_m^2}{\omega^2 - \omega_m^2} \phi_m(z) \, \phi_m'(z_o). \qquad (3\text{-}17)$$

The subscripted terms in the above, ω_m and ϕ_m, depend on the scalar magnitude of $\vec{k}$, while ω is identical to the track component k_x except for the scale factor v, $\omega \equiv k_x v$.

3.3 CROSSPLANE REPRESENTATION

The inversion of the field transform $\overline{\zeta}$ will be carried out in two steps, first analytically along the k_x coordinate to produce the "partial transforms" $\overset{\sim}{\zeta}$,

$$\overset{\sim}{\zeta}(x, k_y, z) = \frac{1}{2\pi} \int_{-\infty}^{\infty} \overline{\zeta}(\vec{k}, z) \, e^{-ik_x x} \, dk_x, \qquad (3\text{-}18)$$

then along the k_y axis

$$\zeta(x, y, z) = \frac{1}{2\pi} \int_{-\infty}^{\infty} \overset{\sim}{\zeta}(x, k_y, z) \, e^{-ik_y y} \, dk_y. \qquad (3\text{-}19)$$

The second step is carried out numerically with the Fast Fourier Transform for a succession of x-values at a given z. As will be seen, the analytic form of the partial transform $\overset{\sim}{\zeta}$ allows it to be assembled rapidly at each x from quantities computed and stored ahead of time.

Each term in the modal sum (3-17) for the field transform contains an integrable singularity along the line of resonance in the $\vec{k}$ plane defined by

24

$$k_x v = \omega_m(k),$$

<div style="text-align: right">(3-20)</div>

$$k^2 = k_x^2 + k_y^2;$$

the finite contribution of these singularities to the inversion integrals constitutes the radiated, freely propagating field. (Singularities occur also along the imaginary k_x axis associated with solutions of the normal-mode equation for negative k^2. These constitute the nonradiated, exponentially-damped field which is the generalization, for stratified flow, of the local potential flow around the source.) Using c_m to denote the scalar phase speed ω_m/k, we note that

$$\frac{k_x}{k} = \frac{\omega_m/v}{k} = \frac{c_m}{v},$$

which indicates that no waves for which $c_m > v$ can be part of the field. It can be shown that c_m is always a decreasing function of k, so that the resonance loci have two possible forms, as shown in Figure 3-1: when $v > c_m(k=0)$ the source is "super-Froude" with respect to the mth mode and the locus leaves the origin at an angle of $\sin^{-1}(c_m(0)/v)$; when $v < c_m(0)$ the locus crosses the k_x-axis at a finite value corresponding to $c_m(k_x) = v$, giving rise to a transverse wave system. While there is no distinction between these two cases in the formalism to follow the inclusion of transverse waves complicates the numerical procedures, and the numerical algorithm has been configured for the super-Froude case only.

To evaluate the radiated contributions we choose the complex integration contour of (3-18) to lie below the real k_x axis so that the field will

MODE 1 SINGULARITY LOCI FOR VARIOUS SOURCE SPEEDS

$v = 0.5$ M/SEC

SUB-FROUDE

0.75 M/SEC

1.0 M/SEC
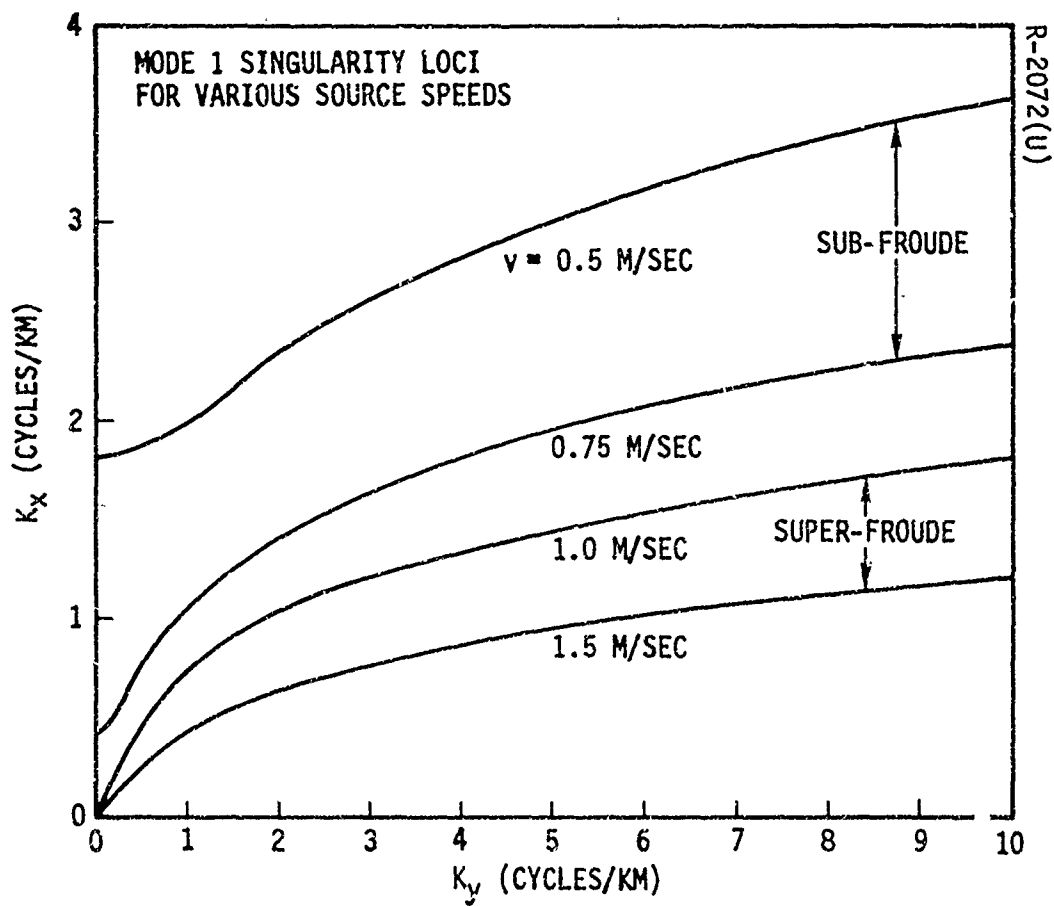
SUPER-FROUDE

1.5 M/SEC

K_x (CYCLES/KM)

K_y (CYCLES/KM)

Figure 3-1. Solution Loci for the Resonance Equation (3-20) at Various Source Speeds. Limiting Phase Speed for Mode 1 is 0.836 M Sec^{-1}.

vanish for $x > 0$, and we include the dependence of ω_m on k_x via k (at fixed k_y) in the computation of the residues,

$$\left[\frac{d}{dk_x}(\omega^2 - \omega_m^2)\right]_{\omega = \pm\omega_m} = 2\omega v - 2\omega_m \frac{d\omega_m}{dk}\frac{dk}{dk_x}$$

$$= \pm 2\omega_m v(1 - c_m c_{gm}/v^2)$$

where $c_{gm} \equiv d\omega_m/dk$ ($\leq c_m$) is the scalar group velocity. The result is

$$\tilde{\zeta}(x,k_y,z) = \pm \frac{iV}{2v} \sum_m c_m^3 k(1 - c_m c_{gm}/v^2)^{-1} \phi_m(z)\ \phi_m'(z_o)\ e^{\mp i\omega_m x/v},$$

$$(3\text{-}21)$$

the sum carried out over both signs.

The numerical procedure is based on the observation that each term $\tilde{\zeta}_m$ of the above sum for the partial transform depends on x only in its complex phase,

$$\tilde{\zeta}_m(x,k_y,z) = T_m(k_y,z)\ e^{-i\omega_m x/v};\qquad (3\text{-}22)$$

the source transform,

$$\boxed{T_m(k_y,z) = \frac{iV}{v} c_m^3 k(1 - c_m c_{gm}/v^2)^{-1} \phi_m(z)\ \phi'(z),}\qquad (3\text{-}23)$$

27

can be computed and tabulated as a function of k_y from the dispersion data and eigenfunction amplitudes. A corresponding table of complex phases

$$e^{-i\omega_m \Delta x/v}$$

can be similarly prepared, after which each $\tilde{\zeta}_m$ can be generated recursively by repeated complex multiplications,

$$\tilde{\zeta}_m(o,k_y,z) = T_m,$$

$$\tilde{\zeta}_m(x + \Delta x,k_y,z) = \zeta_m(x,k_y,z)\, e^{-i\omega_m \Delta x/v}; \qquad (3\text{-}24)$$

at each step the sum

$$\tilde{\zeta}(x,k_y,z) = \mathrm{Re}\left\{\sum_m \zeta_m(x,k_y,z)\right\}, \qquad (3\text{-}25)$$

briefly tabulated as a function of k_y, can be Fourier-transformed to produce $\zeta(x,y,z)$.

Field quantities other than displacement, such as scalar strain, strain rate, and horizontal velocity, can be deduced from the simple relations among the Fourier amplitudes derivable from the dynamical equations (3-1 through 3-4):

$$\text{strain,} \qquad \overline{\epsilon} = -\frac{\partial \overline{\zeta}}{\partial z} = -\overline{\zeta}'$$

$$\text{strain rate,} \qquad \overline{\epsilon}_t = -i\omega\overline{\zeta}'$$

$$\text{velocity,} \qquad \overline{u}_x = \frac{\omega k_x}{k^2}\,\overline{\zeta}' \qquad\qquad (3\text{-}26)$$

$$\overline{u}_y = \frac{\omega k_y}{k^2}\,\overline{\zeta}'$$

For completeness, the appropriately modified formulas for the source transforms are listed below:

Quantity	T_m
ζ	$\dfrac{iV}{v}\,c_m^3 k(1 - c_m c_{gm}/v^2)^{-1}\,\phi_m(z)\,\phi_m'(z_o)$
ϵ	$-\dfrac{iV}{v}\,c_m^3 k(1 - c_m c_{gm}/v^2)^{-1}\,\phi_m'(z)\,\phi_m'(z_o)$
ϵ_t	$\dfrac{V}{v}\,c_m^4 k^2(1 - c_m c_{gm}/v^2)^{-1}\,\phi_m'(z)\,\phi_m'(z_o)$
u_x	$\dfrac{iV}{v^2}\,c_m^5 k(1 - c_m c_{gm}/v^2)^{-1}\phi_m'(z)\,\phi_m'(z_o)$
$u_y^{\,*}$	$\left[\dfrac{ik_y}{k}\right]\dfrac{V}{v}\,c_m^4(1 - c_m c_{gm}/v^2)^{-1}\,\phi_m'(z)\,\phi_m'(z_o)$

(3-27)

---

*The bracketed quantity $[ik_y/k]$ is held outside the sum in Equation 3-25.

29

SECTION 4. WAKE-GENERATED WAVES

4.1 INERT MIXED WAKE

The mixing that occurs within the momentumless wake of a self-propelled body tends to establish a more nearly uniform density in the wake than in the surrounding stratified fluid. Internal waves are radiated as the mixed wake collapses slightly to bring the internal and external density surfaces into level. For radiated components whose wavelength is longer than the wake diameter, the effect of collapse can be reasonably well represented by a time-dependent displacement quadrupole in the crossplane.

To incorporate wake radiation into the present transform algorithm, one approach would be to model the wake collapse separately, either analytically or numerically [7,8] and use the corresponding quadrupole profiles as an additional source term.

A much simpler, though not yet validated, approach has been used in the present version of XMODE. It uses a single parameter in the form of an initial quadrupole strength, and virtually generates the entire quadrupole history in a self-consistent dynamical way as the radiation field develops.

The inert mixed wake, in its simplest conception, is a tube of fluid which, at a suitable short distance behind the self-propelled body, has an anomalous density gradient within an approximately circular cross-section, no mean flow perpendicular to the axis, and in which turbulent stresses can be neglected in comparison to buoyant forces and inertia in the equations of crossplane flow. This last assumption means that the dynamics of collapse are adequately described by the homogeneous equations of fluid motion, both inside and outside the mixed region.

We assume that the only effect of mixing is to redistribute density and we define a displacement function to describe the redistribution,

$$\Delta\zeta(x,y,z-z_o),$$

such that if the mixing were abruptly terminated at position x, a fluid particle on the streamline originally at level z would rise or fall to the new equilibrium level $z+\Delta\zeta$. Thus, if the streamline is at the level $z+\zeta$, the particle experiences an acceleration due to buoyancy $-N^2(\zeta-\Delta\zeta)$. The function $\Delta\zeta$ vanishes for $x>o$, changes rapidly in a mixing interval $-X<x<o$, then remains independent of x for $x<-X$. The vertical momentum equation (3-1) is accordingly modified to read

$$\ddot{\zeta} + \frac{\partial p}{\partial z} + N^2(z)\ (\zeta-\Delta\zeta) = 0, \qquad (4\text{-}1)$$

and following the derivation of Section 3 with the volume source s set to zero, we get

$$\left(\nabla'^2 + \frac{\partial^2}{\partial z^2}\right)\ddot{\zeta} + N^2\nabla'^2\zeta = N^2\nabla'^2\Delta\zeta, \qquad (4\text{-}2)$$

where again the steady solution obeys $\ddot{\zeta} = v^2(\partial/\partial x)^2\zeta$. For simplicity we assume that the turbulent redistribution of density occurs rapidly enough compared to the time scales $\{\omega_m^{-1}\}$ to be approximated by impulsive change,

$$\Delta\zeta = \begin{cases} 0, & x \geq 0 \\ \\ \Delta(y, z - z_o), & x < 0, \end{cases} \qquad (4\text{-}3)$$

which gives the source term in (4-2) the form

$$N^2\left[\eta(x)\ \frac{\partial^2\Delta}{\partial y^2} - \zeta'(x)\Delta\right]$$

where $\eta(x)$ is unity for $x \leq 0$ and zero for $x > 0$. The two-dimensional Fourier transform of this equation is

$$\frac{\partial^2 \bar{\zeta}}{\partial z^2} + k^2 \left(\frac{N^2}{\omega^2} - 1\right) \bar{\zeta} = -\frac{N^2}{\omega^2}\left(\frac{ik_y^2}{k_x} + ik_x\right) \hat{\Delta}(k_y, z - z_o)$$

or,

$$\left[\frac{\partial^2}{\partial z^2} + k^2 \left(\frac{N^2}{\omega^2} - 1\right)\right]\bar{\zeta} = \frac{N^2 k^2}{ik_x \omega^2} \hat{\Delta}(k_y, z - z_o). \qquad (4\text{-}4)$$

In terms of the Green's Function in (3-12), the solution is

$$\bar{\zeta} = \frac{k^2}{ik_x \omega^2}\int G_{k,\omega}(z, z_1)\hat{\Delta}(k_y, z_1 - z_o) \, dz_1$$

$$= \frac{1}{ik_x} \sum_m \frac{\omega_m^2}{\omega^2 - \omega_m^2} \phi_m(z) \, Q_m(z_o), \qquad (4\text{-}5)$$

with

$$Q_m(z_o) = -\int \phi_m(z) N^2(z)\hat{\Delta}(k_y, z - z_o) \, dz. \qquad (4\text{-}6)$$

Now for a range of wavenumbers k_y and mode numbers m such that the spatial scales of the plane-wave normal modes are much larger than the wake radius R,

33

$$k_y R < 1,$$

$$mR < Z_a,$$

the coefficients above are approximately

$$Q_m = \phi_m'(z_o)N^2(z_o)\iint (z_o - z)\Delta(y, z - z_o)\ dydz$$

$$\equiv \phi_m'(z_o)N^2(z_o)Q, \tag{4-7}$$

where the integral Q defines the wake quadrupole moment. This approximation assumes also that the ambient Vaisala frequency is constant over the wake height and that the wake is axisymmetric so that

$$\iint \Delta\ dxdy = 0.$$

The solution transform is thus

$$\overline{\zeta}(\vec{k}, z) = \frac{QN^2(z_o)}{ik_x} \sum_m \frac{\omega_m^2}{\omega^2 - \omega_m^2}\ \phi_m(z)\phi_m'(z_o). \tag{4-8}$$

The partial inversion of Section 3.3 yields the crosstrack transform

$$\tilde{\zeta}(x, k_y, z) = \frac{1}{2}\ QN^2(z_o) \sum_m (1 - c_{gm}c_m/v^2)^{-1}\ \phi_m(z)\ \phi_m'(z_o)\ e^{\mp i\omega_m x/v},$$

$$\tag{4-9}$$

the sum again including both signs of $i\omega_m$. This sum, representing the radiated field, does not include the residue of the singularity at $k_x = 0$, which merely reproduces the impulsive density jump $\Delta\zeta$ inside the wake at $x = 0$.

The source transforms T_m generated by the quadrupole wake are accordingly

Quantity	T_m
ζ	$QN_o^2(1 - c_{gm}c_m/v^2)^{-1} \, \phi_m(z) \, \phi_m'(z')$
ε	$-QN_o^2(1 - c_{gm}c_m/v^2)^{-1}\phi_m'(z) \, \phi_m'(z_o)$
ε_t	$-QN_o^2 i\omega_m(1 - c_{gm}c_m/v^2)^{-1} \, \phi_m'(z) \, \phi_m'(z_o)$
u_x	$QN_o^2 \dfrac{c_m^2}{v} (1 - c_{gm}c_m/v^2)^{-1} \, \phi_m'(z) \, \phi_m'(z_o)$
u_y	$-QN_o^2 \left[\dfrac{ik_y}{k}\right] ic_m(1 - c_{gm}c_m/v^2)^{-1} \, \phi_m'(z) \, \phi_m'(z_o)$

$$(4\text{-}10)$$

4.2 SIZING THE QUADRUPOLE MOMENT

For a considerable range of horizontal and vertical wavenumber the radiation emanating from a collapsing wake is seen to be determined by a single constant, the kinematic quadrupole moment

$$Q = \iint (z_o - z) \, \Delta(y, z - z_o) \, dzdy. \qquad (4\text{-}11)$$

The magnitude of this quantity depends both on the cross section of the mixed wake and on the degree of mixing, as reflected by the density level displacements Δ. There is probably no simple substitute for a complete finite-difference simulation of the turbulent dynamics of wake growth and collapse in stratified media if accurate values of Q are essential. However, certain bounding approximations can be made in anticipation of these more accurate simulations, and a quadrupole formula based on these approximations has been included in the XMODE algorithm.

The estimate derived below is based in an elementary way on the dynamical picture of a growing, momentumless wake given by Ko [9], with constants drawn from the measurements of Naudascher and Gran [10,11]. The procedure will be to assume that in the initial growth stage the density is turbulently diffused like a passive variable, and that the consequent growth in the quadrupole moment continues until the effects of stratification intervene rather abruptly at about one-fourth of the local Vaisala period. In Ko's account of non-stratified growth, the wake radius R and turbulent velocity scale u' depend on time, or downtrack coordinate x, according to

$$R \sim x^{1/4}$$

$$u' \sim x^{-3/4}$$

(4-12)

with a Reynolds stress that is given by an eddy diffusivity

$$\varepsilon = K_\varepsilon u'R \qquad (4-13)$$

that is constant across the wake. In Gran's measurements this assumption is verified, although the exponents in (4-12) are modified very slightly by the effects of propeller-induced swirl. Gran's measurements also

36

verify another assumption of Ko's, that the wake entrainment rate $\dot{R} \equiv vdR/dx$ is proportional to u',

$$\dot{R} = K_1 u'. \tag{4-14}$$

To define the density distribution inside the growing wake we will neglect the effect of swirl and we will suppose, following a Reynolds' analogy, that the diffusion of the passive quantity ρ is governed by the eddy diffusivity ε,

$$\overline{u}_x \frac{\partial \rho}{\partial x} + \nabla \cdot (\varepsilon \nabla \rho) = 0 \tag{4-15}$$

with a boundary condition that equates the normal flux of ρ across the expanding wake perimeter at R:

$$\rho_i \dot{R} + \varepsilon \frac{\partial \rho_i}{\partial n} = \rho_o \dot{R}, \tag{4-16}$$

where $\overline{u}_x$ is the mean longitudinal flow and the subscripts (i,o) mean inside and outside the wake perimeter. The outside density profile is assumed linear,

$$\rho_o = \rho_o(z_o) - \beta(z - z_o). \tag{4-17}$$

These equations have the remarkably simple solution

$$\rho_i = \rho_o(z_o) - \alpha(z - z_o), \tag{4-18}$$

as pointed out by Fernandez [12], since ε depends only on x but $\partial \rho_i / \partial x = 0$ so that (4-15) is satisfied, while the boundary condition becomes

37

$$\alpha(R\cos\theta)\, K_1 u' + K_\epsilon u' R(\alpha\cos\theta) = \beta(R\cos\theta) K_1 u'$$

where θ is the polar angle with $z - z_0 = R\cos\theta$, the condition is everywhere satisfied when

$$\alpha(K_1 + K_\epsilon) = \beta K_1. \qquad (4\text{-}19)$$

This argument suggests that the growing, non-radiating wake maintains a constant internal density gradient whose value is smaller than the external gradient by an amount that depends quite reasonably on the ratio of entrainment constant K_1 to eddy diffusion constant K_ϵ.

The displacements Δ in density surface levels inside the wake are immediately given by

$$\alpha(z - z_0) = \beta[(z - z_0) + \Delta],$$

or

$$\Delta = \frac{\alpha - \beta}{\beta}\,(z - z_0). \qquad (4\text{-}20)$$

The quantity $(\beta - \alpha)/\beta = E$ is a measure of the mixing efficiency,

$$\boxed{\begin{array}{c} \Delta = -E(z - z_0) \\[2mm] E = \dfrac{K_\epsilon}{K_1 + K_\epsilon}, \end{array}} \qquad (4\text{-}21)$$

such that E tends to unity for $K_\epsilon \gg K_1$ and to zero for $K_1 \gg K_\epsilon$.

The kinematic quadrupole moment (4-11) is readily found to be

$$Q = \frac{\pi R^4}{4} E, \qquad (4-22)$$

which is seen to grow linearly with time in view of the $x^{1/4}$-dependence of R. The value for R taken from Gran's results for a streamlined body-and-propeller model of radius R_b yields

$$R^4 \doteq R_o^4 \left[0.213\left(\frac{x - x_o}{2R_b}\right) \right]$$

where $R_o = 1.19\ R_b$ is the value at $x = 12\ R_b$ and x_o is a virtual origin a short distance ($2.6\ R_b$) in front of the propeller. Assuming that quadrupole growth terminates abruptly after some fraction f of the Vaisala period, when

$$x - x_o = f\frac{2\pi v}{N_o},$$

we get for the maximum quadrupole

$$\boxed{Q = 0.26\ ER_b^3\ v/N_o.} \qquad (4-23)$$

This is the formula implemented in the SOURCE module, with the mixing efficiency E as a variable input parameter, and with the number f taken as 0.25. The appropriate value of E can be inferred from formula (4-21); values of K_1 and K_ε taken by Ko from Naudascher's measurements, and computed by Gran from his own data [13], yield roughly similar values of E:

39

	Gran	Naudascher
K_ε	0.16	0.18
K_1	2.3	2.25
E	0.064	0.074

Both values of E are small enough to suggest that the actual mixing tha occurs in a propeller wake may be dominated by gross convection due to swirl. Gran remarks that a core of the wake extending out to $\simeq 0.25\,R$ remains in solid body rotation and attains 0.8 revolutions after 20 body diameters. If the portion out to 0.5 R were completely mixed, the equivalent added mixing efficiency would be on the order of $(0.5)^4 = 0.0625$.

4.3 TREATMENT OF HIGHER MODES

The approximation (4-7) for the mode-dependent quadrupole coefficients (4-6) overemphasizes the higher modes and higher wavenumbers by treating the source like a point quadrupole singularly in the crossplane. The normalized mode product $\phi_m' \phi_m'$ appearing in the source transform formulas for strain, velocity, and strain rate is on the average an increasing function of m, of order

$$\phi_m' \phi_m' \sim p_m^2 \int \phi_m^2 \, dz \equiv \frac{p_m^2}{N_m^2},$$

where one defines a vertical wavenumber p_m by

$$p_m^2 \int \phi_m^2 \, dz \equiv \int \phi_m'^2 \, dz$$

and a mode-averaged N^2 by

$$N_m^2 \int \phi_m^2 \, dz = \int \phi_m^2 N^2 dz = 1.$$

40

One can easily derive from the normal-mode equation (3-10) the relation

$$k^2 + p_m^2 = c_m^{-2} N_m^2,$$ (4-24)

so that the wake-generated source transforms for strain,

$$T(\text{wake}) \sim Q N_o^2 c_m^{-2} (1 - \frac{\omega_m^2}{N_m^2})$$

tend to grow without mode limit. The extra factor $c_m^3 k$ in the body-generated source transforms attenuates these functions at higher mode numbers. This behavior is evident in the body-dominated and wake-dominated cases illustrated in Figures 2-5 and 2-6 .

The actual wake excitation coefficients defined in equation (4-6) will diminish with increasing k and m at a point where the scale of the mode function becomes comparable to the maximum wake radius R. A simple form factor to simulate this effect qualitatively has been included in the wake transform algorithm,

$$\frac{1}{1 + 0.4\, q_m^2\, R^2},$$ (4-25)

where q is a total wavenumber defined by

$$q_m^2 = k^2 + p_m^2,$$ (4-26)

and computed very simply from quantities on hand by formula (4-24) above.

41

REFERENCES

1. M. Milder, User's Manual for the Computer ZMODE, R & D Associates, Report TR-2701-001, July 1973.

2. G. Carrier and A. Chen, Internal Waves Produced by an Underwater Vehicle, TRW, Inc., Report No. 18202-6001-RO-00, November 1971.

3. C. W. Hirt and D. R. S. Ko, personal communication.

4. J. W. Cooley and J. W. Tukey, "An Algorithm for the Machine Computation of Complex Fourier Series," Math. of Comp., Vol. 19, April 1965, pp. 297-301.

5. J. W. Miles, "Internal Waves Generated by a Horizontally Moving Source," Geo. Fluid Dynamics, Vol. 2, 1971, pp. 63-87.

6. O. Phillips, The Dynamics of the Upper Ocean, Cambridge University Press, 1969, pp. 164-165.

7. D. R. S. Ko, Collapse of a Turbulent Wake in a Stratified Medium, TRW, Inc., Report 18202-6001-RO-00, Vol. II, November 1971.

8. S. A. Piacsek, NRL Report pending.

9. D. R. S. Ko, A Phenomenological Model for the Momentumless Turbulent Wake in a Stratified Medium, TRW, Inc., Report 20086-6007-RU-00, April 1973.

10. E. Naudascher, "Flow in the Wake of Self-Propelled Bodies and Related Sources of Turbulence, JFM, Vol. 22, 1965, pp. 625-656.

11. R. L. Gran, An Experiment on the Wake of a Slender Propeller-Driven Body, TRW, Inc., Report 20086-6006-RU-00, June 1973.

12. F. L. Fernandez, R & D Associates, personal communication.

13. R. L. Gran, Flow Research, Inc., personal communication.